ACS OMEGA

http://pubs.acs.org/journal/acsodf

Article

Synthesis and Emergent Photophysical Properties of Diketopyrrolopyrrole-Based Supramolecular Self-Assembly

Nilabja Maity, Kanad Majumder, Arun Kumar Patel, Diptikanta Swain, Nagarajarao Suryaprakash, and Satish Patil*

Cite This: *ACS Omega* 2022, 7, 23179−23188

Read Online

ACCESS | Metrics & More | Article Recommendations | Supporting Information

ABSTRACT: Diketopyrrolopyrrole (DPP)-based molecular semiconductors exhibit intriguing optical and charge transport properties. Herein, we rationally design a series of electronically identical but structurally distinct Hamilton receptor (HR)-based supramolecular assembly of DPP. The HR endows supramolecular assemblies via hydrogen bonding with enhanced structural ordering and excitonic couplings. The mechanism of supramolecular self-assembly was probed by diffusion ordered spectroscopy (DOSY) nuclear magnetic resonance (NMR) and solid-state IR spectroscopy studies. We investigated the morphology of self-assembly, photophysical and electrochemical properties and compared them with the identical DPP molecular structures without HRs. The microstructure of self-assembly was probed with atomic force microscopy in thin films. Subsequently, the influence of solid-state packing was studied by single-crystal X-ray diffraction. The single-crystal structure of HR-TDPP-C_{20} reveals slipped stack arrangements between the two neighboring chromophores with $\pi-\pi$ stacking distance and slip angle of 3.55 Å and 35.4°, respectively. Notably, the slight torsional angle of 1° between thiophene and lactam rings and small $\pi-\pi$ stacking distance suggest a significant intermolecular coupling between thiophene (D) and lactam (A) rings. This intramolecular coupling between two $\pi-\pi$ chromophore stacks manifests in their optical properties. In this manuscript, we report rational design and synthesis of supramolecular self-assembly of DPP with a collection of compelling structural and optical properties.

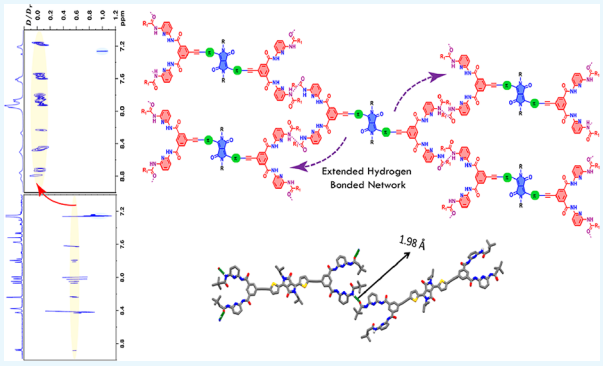

1. INTRODUCTION

The supramolecular self-assembly of π-conjugated molecules exhibits enhanced $\pi-\pi$ interactions and electronic coupling by bringing discrete building blocks together.[1] As a result, these materials display significant improvement in structural order and show remarkable applications in the field of flexible optoelectronic devices, self-healing materials, and biomedical applications.[2−10] The emergent field of supramolecular chemistry was introduced by Jean−Marie Lehn in the 1990, invoking interactions of non-covalent chemical bonds.[11,12] The concept was inspired by the ubiquity of intermolecular processes in naturally occurring light-harvesting photosynthetic units, DNA and RNA genetic materials.[13−16] However, decrypting the mechanism of supramolecular polymerization was a topic of debate even after prolonged research.[17,18] Meijer et al. acquired incredible ensemble of results toward understanding the complex mechanism of supramolecular polymerization and proposed a rational definition for supramolecular polymers as "polymeric arrays of monomeric units that are brought together by reversible and highly directional secondary interactions, resulting in polymeric properties in dilute and concentrated solution as well as in bulk."[18−21] Meijer and co-workers also demonstrated remarkable mechanical properties of supramolecular polymers as robust as covalently linked repeating units in conventional polymers, since then the field has evolved immensely.[22−28] Moreover, a wide range of ordered supramolecular polymers have been studied to explore the potential application in the field of unidirectionally charge transport over a long distance, including molecular systems of hexabenzocoronene (molecular graphene), oligo(*p*-phenylene vinylene), perylene bisimide, and naphthalene diimides.[29−40]

In the recent past, donor−acceptor (D-A-D) π-conjugated polymers have shown promising properties in optoelectronic devices.[41−45] In D-A-D polymers, the electronic coupling is modulated by the donor and acceptor interaction through a π-conjugated bridge. Delocalization of charge in the D-A-D system is governed by alternating electron-donating and electron-accepting units due to the push−pull mechanism. In

Received: February 23, 2022
Accepted: June 14, 2022
Published: June 30, 2022

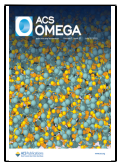

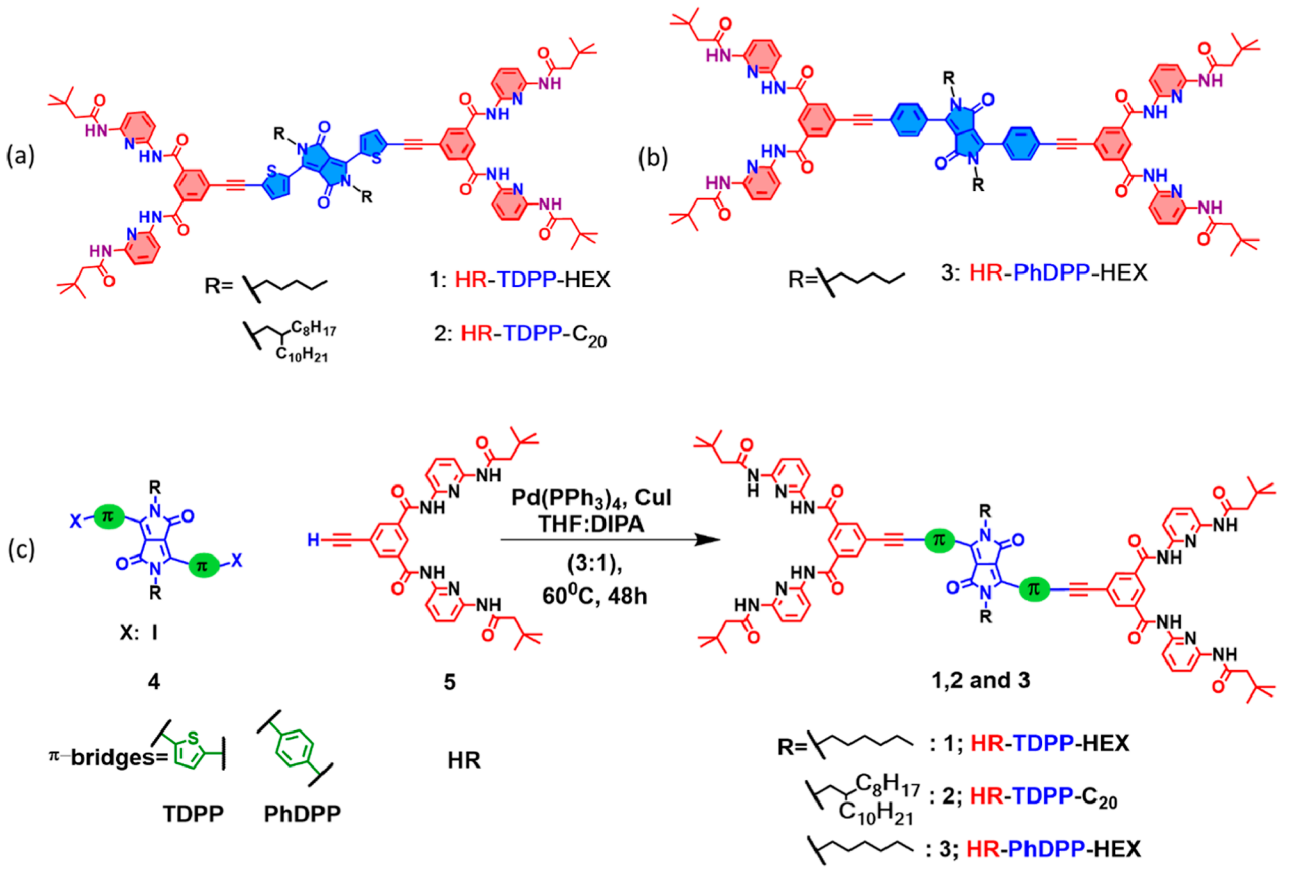

Figure 1. Chemical structure of DPP-based supramolecules (a) HR-TDPPs 1−2 and (b) HR-PhDPP 3. (c) Synthetic scheme of HR-DPP molecules.

addition, such chromophores exhibit a broad dual band absorption spectrum with intermolecular charge transfer and large dipole moments within the π-conjugated backbone.[46] Such materials have shown low energetic disorder, high charge-carrier mobility in organic field-effect transistors (OFETs), and record efficiency in organic photovoltaic devices (OPVs).[47,48] In addition, the D-A-D system has also shown promising applications in non-linear optics such as two/three-photon absorptions.[49−52]

Among the family of D-A-D π-conjugated polymers, the diketopyrrolopyrrole (DPP) unit served as an excellent electron acceptor and attracted a great deal of attention not only for their outstanding photophysical and optoelectronic properties but also for their self-assembly properties.[53−65] The molecular structure of DPP contains a planar conjugated backbone and a cyclic amide functional group, which can be substituted with a variety of alkyl chains.[66] In addition, the substituted DPP with the appropriate donor group shows high thermal stability, fluorescent quantum yield, and exhibit enhanced charge-carrier mobility. In recent years, DPP derivatives have shown a potential application in the field of molecular-based optoelectronic devices such as organic electrochemical transistors (OECTs),[73] organic thermoelectric materials (OTEs),[72] OFETs,[69−71] and OPVs.[67,68] In search of ambipolar organic semiconductors, our group has developed a novel series of DPP-based alternating copolymers.[74−78] Surprisingly, simple molecular engineering has led to a remarkable improvement in electron mobility (~3 $cm^2V^{-1}s^{-1}$) in OFETs and acts more like conventional inorganic semiconductors with a band-like transport.[79,80] Till date, Ajayaghosh and co-workers demonstrated 2D nanosheets of the self-assembly layer under organic and aqueous conditions by substituting hydrophilic and hydrophobic groups with DPP,[81] showing a anisotropic charge-carrier mobility of 0.33 $cm^2\ V^{-1}\ s^{-1}$.

Inspired by DPP's unique optical and charge transport properties, in this work, we rationally combined the DPP molecular backbone with a terminal functional group of the Hamilton receptor (HR). The complementary intermolecular hydrogen bonding of the HR was earlier reported by Lehn and co-workers.[82−86] In our rational approach, we have introduced planar thiophene moiety of DPP, substituted with two different alkyl chains, *n*-hexyl (HR-TDPP-HEX) and 2-octyldodecyl (HR-TDPP-C_{20}). In addition, we introduced twist in the backbone with the phenyl group (HR-PhDPP-HEX) attached with C3 and C6 positions of the DPP core.[87] The genericity of such a design strategy is to (i) combine multiple hydrogen bonds of the HR to increase the strength of non-covalent interactions via supramolecular polymerization, (ii) manipulate excitonic coupling by twisting the backbone of DPP, and (iii) gain structural order via supramolecular self-assembly. We observed intriguing optical and structural properties such as reversible supramolecular self-assembly, ordered microstructures, and enhancement in intermolecular excitonic coupling. We established the role of intermolecular hydrogen bonding by the concentration-dependent ^{1}H NMR study, whereas the variable temperature ^{1}H NMR study reveals the reversible nature of polymerization. A notable difference observed in the relative diffusion coefficient in the two-dimensional diffusion-ordered spectros-

https://doi.org/10.1021/acsomega.2c01091
ACS Omega 2022, 7, 23179−23188

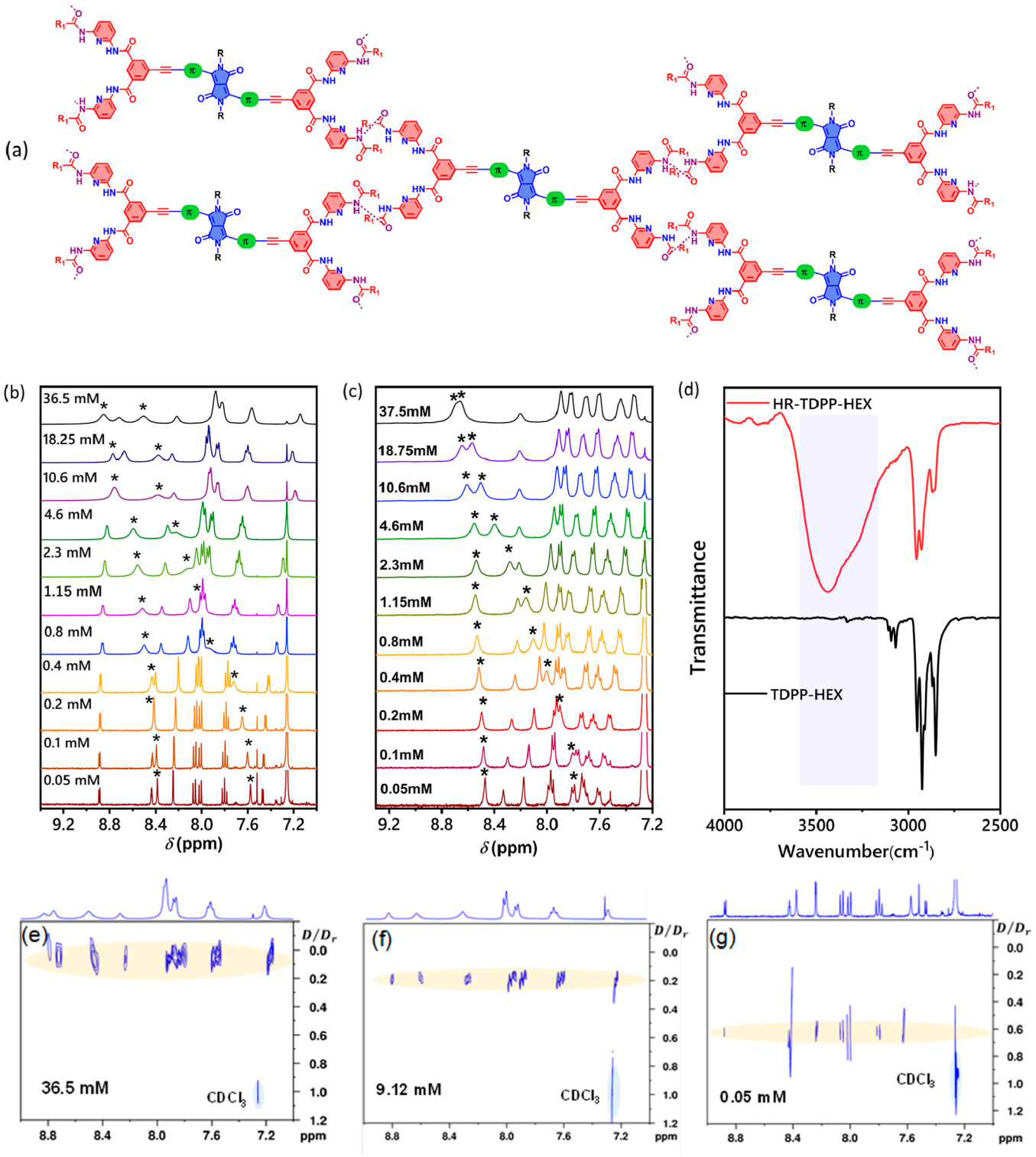

Figure 2. (a) Schematic illustration of the supramolecular polymerization of DPPs via self-complementary hydrogen bonding (−NH...C═O−) through the HR. Concentration-dependent ^{1}H NMR spectra of (b) HR-TDPP-C_{20} and (c) HR-PhDPP-HEX molecules in $CDCl_3$ solvent at room temperature. A concentration-dependent systematic shift of amide protons (star mark) of the HR. (d) FT-IR spectra of HR-TDPP-HEX and TDPP-HEX. (e−g) 2D-DOSY spectra at different concentrations of HR-TDPP-C_{20} molecule at room temperature. Diffusion coefficients of supramolecular polymers are given in Supporting Information (Table S3) relative to the diffusion coefficient (D/D_r) of the internal reference $CDCl_3$.

copy (2D-DOSY) nuclear magnetic resonance (NMR) experiment suggests the formation of supramolecular polymers. Based on these experimental studies, we report synthesis of a new family of DPP-based supramolecular self-assembly with a detailed mechanistic study on the origin of supramolecular polymerization, reversible self-assembly, and persuasive photophysical properties.

https://doi.org/10.1021/acsomega.2c01091
ACS Omega 2022, 7, 23179−23188

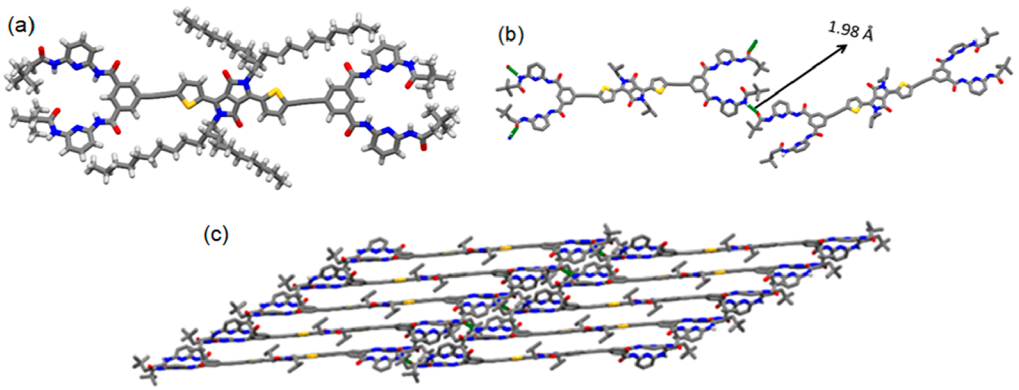

Figure 3. X-ray structure of HR-TDPP-C_{20} in capped stick representation. (a) Front view with the alkyl chain. (b) Intermolecular hydrogen bonding through N−H...O═C (green) interactions in the HR. (c) Supramolecular polymerization growth via intermolecular hydrogen bonding. (b,c) Alkyl chains and hydrogen atoms are omitted for clarity.

2. RESULTS AND DISCUSSION

2.1. Design and Synthesis. The basic molecular structure contains a DPP core with two different π-bridges, planar thiophene and the twisted phenyl moiety. The DPP core is covalently linked with the HR, which undergoes polymerization via self-complementary H-bonding, as shown in Figure 2a. To investigate further the role of the alkyl chain in supramolecular packing, we have substituted −NH− of the lactam ring with "two different alkyl chains, that is, hydrophobic *n*-hexyl (HEX) and bulky soluble hydrophobic 2-octyl dodecyl (C_{20}) groups. The synthetic scheme for the DPP derivatives, HR-TDPP-HEX (1), HR-TDPP-C_{20} (2), and HR-PhDPP-HEX (3), is shown in Figure 1a,b. They were synthesized via Sonogashira C−C, cross-coupling reactions involving appropriate monomers having acetylene functionality HR (2.2 equiv) and respective di-iodo derivatives of N-alkylated DPP (1 equiv) in the presence of the palladium catalyst $Pd(PPh_3)_4$ with an activating catalyst CuI in tetrahydrofuran and di-isopropylamine mixture (3:1; v/v) medium (Figure 1c). The HR was synthesized according to the reported procedure with necessary modifications. The detailed synthetic procedures and structural characterization of the final products were carried out using ^{1}H and ^{13}C NMR spectroscopies and MALDI-MS (extended data in Supporting Information). The newly synthesized supramolecules are named as HR-TDPP-HEX, HR-TDPP-C_{20}, and HR-PhDPP-HEX by the molecular components involved in the backbone.

2.2. Spectroscopic Investigation of Supramolecular Polymerization. Spectroscopic studies focused on the mechanism of supramolecular polymerization. To understand the mechanism of polymerization, a series of NMR experiments were carried out, viz. Concentration dependent, variable temperature, and 2D-DOSY in solution. The nature of H-bonding in the HR-TDPP-C_{20} molecule was investigated in detail by concentration-dependent ^{1}H NMR. When the concentration of HR-TDPP-C_{20} increased from 50 μM to 36.5 mM, the well-resolved amide peaks in the aromatic region shifted downfield gradually and converged into a broad spectrum, suggesting the presence of intermolecular hydrogen bonding (Figure 2b). The peak assignment of the aromatic region is shown in Figure S3. These results also reveal that the supramolecular polymers via the self-complementary intermolecular hydrogen bonding network could be constructed at high concentrations. Upon dilution, amide proton shifted upfield (Figure 2b), and a similar trend was also observed in HR-PhDPP-HEX molecules (as shown in Figure 2c). At a very high concentration in HR-TDPP-C_{20} (36.5 mM), the two broad peaks at 8.87 and 8.54 ppm and the peaks resonating at 137.9 and 145.3 ppm (^{15}N−^{1}H HSQC, heteronuclear single quantum coherence spectra) refer to the unsymmetrical two-amide protons (total four in each HR) involved in intermolecular hydrogen bonding, as shown in Figures 2b and S5d. To further understand the mechanism of polymerization, we have also conducted the two-dimensional nuclear Overhauser effect spectroscopy (NOESY) NMR experiment. The correlation peak at 8.4 ppm in HR-TDPP-C_{20} (10.6mM) refers to the spatial proximity between the terminal amide and HR $-CH_2$ protons as they are approaching through intermolecular hydrogen bonding (Figures 2a and S5e,f). While the core amide protons at 8.73 ppm show a significant correlation with water molecules, which is also concluded from the single-crystal X-ray diffraction structure (as discussed later). These results suggest that the supramolecular polymers are formed via intermolecular hydrogen bonding of the HR involving amide and neighboring carbonyl groups.

To further substantiate the formation of supramolecular polymers, 2D-DOSY[88,89] experiments were performed at different concentrations in $CDCl_3$ solution, as shown in Figure 2e−g. A significant difference in diffusion values at different concentrations in $CDCl_3$ solution was observed. The high concentration (36.5 mM) of HR-TDPP-C_{20} exhibits a low value of the relative diffusion coefficient[90] (0.034), which suggests the formation of an aggregate with large hydrodynamic diameter and results into sluggish motion in solution. The notable difference in the diffusion coefficient $D = 2.66 \times 10^{-10} m^2 s^{-1}$ at high (36.5 mM) and $D = 1.55 \times 10^{-9} m^2 s^{-1}$ and low concentrations (50 μM) clearly ascertains that the supramolecular polymerization occurred through intermolecular hydrogen bonding via the HR (Table S3).

To further establish the role of hydrogen bonding in supramolecular polymerization of DPP, we conducted Fourier-transform infrared (FT-IR) spectroscopy studies. As shown in Figure 2d, the FT-IR spectra in the high-frequency region is dominated by a broad peak at 3165 to 3600 cm^{-1}, associated with −N−H groups forming hydrogen bonds with C═O groups of HR-DPP. However, non-hydrogen-bonded inner amide N−H shows signature peak at wavenumber (~3500 cm^{-1}), overlapped with the hydrogen bonded region. To identify these peaks, a deconvolution of the region to

https://doi.org/10.1021/acsomega.2c01091
ACS Omega 2022, 7, 23179−23188

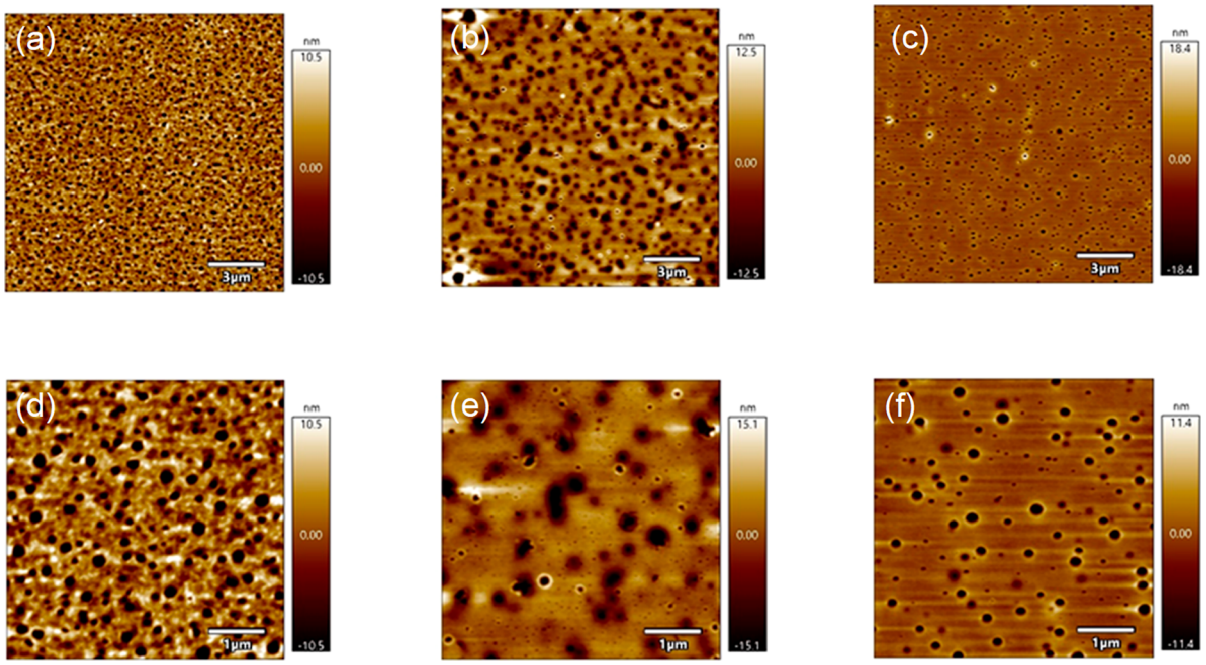

Figure 4. AFM height images of 15 × 15 μm for (a) HR-TDPP-HEX, (b) HR-TDPP-C_{20}, and (c) HR-PhDPP-HEX. (d–f) Corresponding 5 × 5 μm height images.

different peaks are shown in Figure S6c-e. Such broad peaks in the high-frequency region are not observed for the DPP sample without HR (Figures 2d and S6). Combined studies of NMR and FT-IR clearly established the role of the HR for supramolecular polymerization.

The reversible nature of the supramolecular polymer was investigated by the variable temperature studies. A concentrated solution (10.6 mM) of HR-TDPP-C_{20} in $CDCl_3$ was taken for the temperature variation study to observe the reversible nature of polymerization. The NMR spectra of HR-TDPP-C_{20} exhibit broad and multiple peaks at various heating and cooling temperature cycles (see Figure S2). A broad peak in the aromatic region primarily arises due to the formation of aggregates upon decreasing the temperature. It is particularly noteworthy that the peaks in the forward and reverse heating cycles are superimposable. These results suggest that the formation of supramolecular polymers formed via hydrogen bonds is prevalent and reversible in nature in response to temperature.

2.3. Crystal Structure. The mode of non-covalent interactions responsible for supramolecular polymerization is further established by single-crystal XRD. Among the three derivatives, single crystal of HR-TDPP-C_{20} was obtained in chlorobenzene via a slow evaporation method. The crystallographic details are summarized in Table S1 (see Supporting Information). Analysis of the crystal structure reveals that the molecule crystallizes in the monoclinic lattice with a space group I2/a and $Z = 4$, an inversion symmetry concerning two thiophene groups. The two thiophene remains *trans*-oriented with a small torsion angle of 1° with the lactam ring core of the DPP (Figure 3a and S7). Notably, the initial part of the receptor, that is, acetylene bridge aryl, remains planar with the lactam core (Figure S7). The molecule crystalizes with residual four water molecules in hydrogen bonding. The free amide group (terminal two amide) in the HR part plays a crucial role in extended intermolecular H-bonding (Figure 3b,c). The HR-TDPP-C_{20} exhibits slip-stack or head-to-tail 2D layer structures due to intermolecular H-bonding between the amide functional group in HR, locking the orientation. Interestingly, only the terminal amide participates in self-complementary hydrogen bonding with the neighboring chromophore HR group via N–H...O=C interaction, and the intermolecular hydrogen bonding distance is 1.98 Å (Figure 3b). Therefore, each chromophore can hold a side-by-side four chromophore and forms an extended 2D supramolecular polymer network in a solid state. Therefore, each layer slipped away from each other by the angle of 32°, and the shortest $\pi-\pi$ stacking distance is 3.55 Å. Also, the diagonal distance between the two-mass center (R) is 8.3 Å. The crystal structure truly represents the role of the HR for initiate the polymerization and providing non-covalent interaction functional groups to obtain a unique 2D solid-state structure.

2.4. Microscopic Structure (AFM). The thin-film morphology of supramolecular polymers was examined with tapping mode atomic force microscopy (AFM). The thin films were prepared on a silicon wafer by drop-casting a dilute solution (0.25 mg/ml) of molecules in the chloroform solvent. As shown in Figure 4, the height image clearly shows a drastic change in the morphology of the self-assembled microstructure by varying the side chain or twist in the DPP lactam ring. Notably, HR-TDPP-HEX exhibits microfibers with a densely interconnected network. Similarly, HR-TDPP-C_{20} and HR-PhDPP-HEX do not form such well-ordered structures; however, they show a self-assembled layer structures with 10–20 nm, consisting of periodic distribution of pinholes. The presence of a short alkyl chain and extended network of intermolecular hydrogen bonding makes HR-TDPP-HEX molecule a perfect candidate for order supramolecular microstructure. From the microscopic observation, it is distinctly evident that a change in the side chain or incorporating twist in the bridge provides a drastic change in molecular packing, leading to the morphological variation in supramolecular self-assembly of these derivatives.

https://doi.org/10.1021/acsomega.2c01091
ACS Omega 2022, 7, 23179–23188

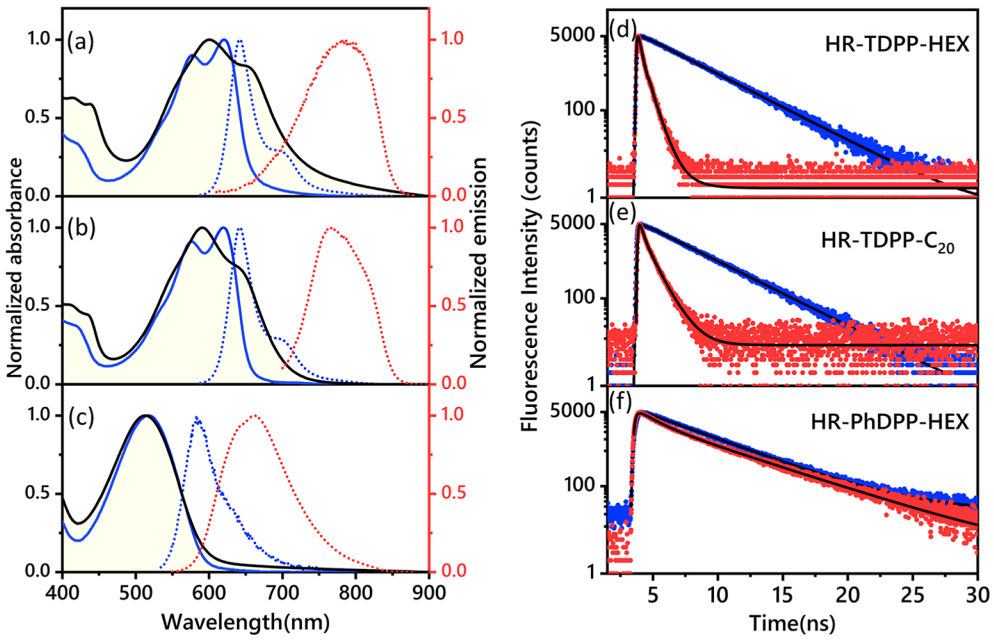

Figure 5. Absorption and emission spectra of HR-DPP molecules in solutions and thin films; absorption/emission spectra were recorded in chloroform (10×10^{-6} M) solution. Spectra in solid blue and black (light yellow shaded) line stand for corresponding solution and thin-film absorption; blue and red dot lines represent for solution and thin film emission of (a) HR-TDPP-HEX, (b) HR-TDPP-C_{20}, and (c) HR-PhDPP-HEX, respectively. Emission lifetime decay profiles in solution (blue), thin film (red), and fits (black) for the four molecules obtained from the TCSPC measurements. (d) HR-TDPP-HEX, emission collected at 642 and 775 nm for solution and thin films. (e) HR-TDPP-C_{20}, emission collected at 642 and 750 nm for solution and thin films. (f) HR-PhDPP-HEX, emission collected at 586 and 660 nm for solution and thin films.

To establish the role of hydrogen bonding on regulating the morphology, we have probed morphology of DPP derivative without the HR. We have adopted similar experimental conditions of HR-TDPP and preparation method to compare the morphology of thin films. Interestingly, TDPP-HEX, TDPP-C_{20}, and PhDPP-HEX reveal small plate-like crystallites microstructures (Figure S8). We observed a pronounced difference in the morphology of thin films. All three DPP derivatives exhibit lack of periodic microstructures as compared to HR-DPP molecules. This study clearly highlights the importance of non-covalent interactions provided by hydrogen bonding, gaining precise nanostructured morphology in thin films of DPP-based supramolecular self-assembly.

2.5. Optical and Electrochemical Properties. We probed optical properties of the HR-DPP derivatives using UV−visible and photoluminescence (PL) spectroscopy in dilute solution of chloroform. The UV−visible absorption spectra of HR-TDPP-HEX and HR-TDPP-C_{20} are very similar (see Figure 5a,b). This clearly indicates that the side chain does not play any role in electronic coupling of HR-TDPP chromophores. HR-PhDPP-HEX shows a significant blue shift in the peak maxima of 104 nm compared to the HR-TDPP derivative, revealing a substantial difference in intramolecular electronic coupling between the DPP core and phenyl donor. Twist around the aromatic phenyl ring to the lactam plane of 31° (as shown in energy-optimized structure, S10) and the higher aromatic resonance energy of phenyl, compared to the thiophene analogue, lead to the less quinoidal character between the donor−acceptor. This causes a reduction in the effective conjugation length, increased optical band gap, and dwindling in the extinction coefficient of the molecule. The extinction coefficient values for all three molecules are shown in Figure S9 and Table S5. The HR-TDPP derivatives exhibit pronounced vibronic excitation states with dual-band absorption, typical characteristic features of the D-A-D system. However, HR-PhDPP-HEX shows a broad peak, which is consistent with the twist observed in dihedral angle along the π-conjugated backbone. The twist impedes the delocalization of π-electrons, solid-state packing, and electronic coupling. Notably, we observed a bathochromic shift of 71 and 100 nm absorption spectra compared to their corresponding building block TDPP and PhDPP without HR. This clearly reveals that the effective conjugation length of the HR-TDPP chromophores increased due to coupling between the receptor's moiety, that is, acetylene and phenyl (Figure S7d).

Compared to solution spectra, a bathochromic shift and peak broadening are observed in thin-film absorption spectra, indicating strong intermolecular coupling between the chromophores. As shown in Figure 5a,b, the thin-film absorption spectra of HR-TDPP-HEX and HR-TDPP-C_{20} display a bathochromic shift of 33 and 19 nm, respectively. Such a major shift in the absorption spectra was not observed for HR-PhDPP-HEX thin films. These results suggest that both effects, twist in the backbone and side chains, play an important role in determining the nature of exciton band and photophysical response.

The electrochemical properties of the three DPP supramolecules were evaluated using cyclic voltammetry (CV). The CV of three derivatives of HR-DPP are shown in Figure S12. The thiophene derivatives of HR-DPP show a one-electron reversible redox cycle, whereas phenyl derivative HR-PhDPP-HR shows two electrons reversible in the reduction cycle. The lowest unoccupied molecular orbital energy level (LUMO) values were estimated from the onset of the first

https://doi.org/10.1021/acsomega.2c01091
ACS Omega 2022, 7, 23179−23188

Table 1. Photophysical Data of HR-DPP Derivatives[a]

	ΔE_g(optical gap) (eV)		Φ_{fl} (%)		τ_{fl} (ns)		k_r (ns^{-1})	
	solution	thin film	solution	thin film	solution	thin film	solution	thin-film
HR-TDPP-HEX	1.88	1.72	36.14	0.18	2.87	~0.28	0.12	$\sim 6.4 \times 10^{-3}$
HR-TDPP-C_{20}	1.89	1.76	64.65	0.28	2.95	~0.62	0.21	$\sim 4.5 \times 10^{-3}$
HR-PhDPP-HEX	2.10	2.07	77.68	5.70	4.0	3.49	0.19	16.3×10^{-3}

[a] ϕ_{fl}, fluorescence quantum yield; τ_{fl}, fluorescence lifetime; and $k_r = \phi_{fl}/\tau_{fl}$ (ns^{-1}). The optical gap of the molecules is calculated from the absorption spectra red edge(λ_{abs}). $\Delta E_g = 1240/\lambda_{abs}$ eV)

reduced peak, using the ferrocene/ferrocenium (Fc/Fc^+) redox couple as a reference standard (details are shown in the Supporting Information). The highest occupied molecular orbital energy levels were estimated by combining optical band gaps (estimated in thin films) with electrochemically estimated LUMO values, as summarized in Table S2. The electrochemical experiments suggest that these materials are promising candidates for developing n-channel and/or ambipolar field-effect transistors.

2.6. Steady-State Emission and Lifetime Characterization. Excited-state dynamics of the molecule were probed by using time-correlated single-photon counting (TCSPC) measurements. Figure 5a–c shows the steady-state PL spectra obtained in solution and thin films. A far more dramatic effect is observed in the excited-state dynamics. The thiophene derivatives (HR-TDPP-HEX and HR-TDPP-C_{20}) exhibit PL spectra with a minimal Stoke shift of 527 cm^{-1} (Table S5). However, the HR-PhDPP-HEX shows a broad structureless emission band with a significant Stoke shift of 2144 cm^{-1}. The HR-PhDPP-HEX exhibits a high photoluminescence quantum yield (PLQY) of 77%, while HR-TDPP-C_{20} and HR-TDPP-HEX show 64 and 36%, respectively. Although the thiophene derivatives have identical backbones, HR-TDPP-HEX shows high aggregation tendency in chloroform and exhibits less quantum yield than HR-TDPP-C_{20}.

The PL spectra in thin films show a broad emission, significant Stoke shift, and absence of vibronic peak progression in HR-TDPP-HEX, HR-TDPP-C_{20}, and HR-PhDPP-HEX (see Figure 5a–c). In thiophene derivatives, the emission quenched drastically compared to solution. The trend in optical properties is similar to those observed earlier by our group for TDPP-HEX, TDPP-C_{20}, and PhDPP-HEX (see Figure S10).

The excited-state lifetime was measured using TCSPC (Figure 5d–f). The thiophene derivatives in solution (HR-TDPP-HEX and HR-TDPP-C_{20}) exhibit monoexponential decay in both vibronic peaks of the emission, with a lifetime of 2.87 to 3 ns (Table 1). While HR-PhDPP-HEX displays a monoexponential decay with 4 ns at the 586 nm emission peak maximum. This mono exponential component attributes to the singlet exciton emission lifetime of the monomer, as similarly reported for DPP molecules. The decay profiles of all DPP derivatives without HR in thin films are triexponential in nature with an average lifetime of 2 to 5 ns.[75,76] Remarkably, in the thin film, the HR-TDPP-HEX and HR-TDPP-C_{20} shows a considerably small emission lifetime (Figure 5d,e), reflecting the faster radiative rates; however, the decreased PL quantum yield for thin films suggests an increasing non-radiative pathway for decay (k_{nr}). The same quenching was also observed in other emission vibronic peaks (750, 775, and 800 nm). The fluorescence lifetime in thin films is considerably smaller than solution, indicating the presence of a strong competing non-radiative decay pathway such as triplet or CT state formation in thin films. However in HR-PhDPP-HEX, the emission lifetime does not change significantly (3.45 ns). It reveals that the improvement in molecular packing and electron couplings is negligible compared to all thiophene derivatives via supramolecular self-assembly. In summary, such well-ordered supramolecular self-assembly leads to enhanced electronic coupling between molecules in the solid state, which can induce interesting, excited-state phenomena and an efficient pathway for charge transport.

3. CONCLUSIONS

In conclusion, the non-covalent interactions of the HR units tend to add up cooperatively. The π-conjugated backbone and nature of the alkyl chain are key factors, which affect the macroscopic structures. The combination of these factors leads to emergent photophysical properties and hierarchy of structures over range of different length scales. The presence of a slipped stack arrangement between two DPP units and self-complementary intermolecular hydrogen bonding through the amide moiety of the HR was clearly elucidated from the single-crystal XRD structure of HR-TDPP-C_{20}. Notably, each molecule can accommodate four neighboring chromophores by the side via hydrogen bonding through the HR group and forms a two-dimension interconnected network, which can be utilized as an efficient pathway for charge transport. We envisage from the preliminary optical study that such supramolecular self-assemblies could lead to interesting, excited-state dynamics distinct from its monomeric behavior. The rational synthetic strategy demonstrated in this work provides an efficient way to control structural disorder and realize emergent photophysical properties in DPP-based molecular systems.

■ ASSOCIATED CONTENT

Supporting Information

The Supporting Information is available free of charge at https://pubs.acs.org/doi/10.1021/acsomega.2c01091.

Instrumentation details, synthesis details, experimental details, aromatic peak assignment, DOSY, NOESY, $^{15}N-^{1}H$ HSQC, variable temperature ^{1}H NMR, FT-IR, UV–vis spectra, energy-optimized structure, ^{1}H and ^{13}C NMR spectra, MALDI-MS data, TCSPC analysis, and crystal information (PDF)

■ AUTHOR INFORMATION

Corresponding Author

Satish Patil − *Solid State and Structural Chemistry Unit, Indian Institute of Science, Bangalore 560012, India;* orcid.org/0000-0003-3884-114X; Email: spatil@iisc.ac.in

https://doi.org/10.1021/acsomega.2c01091
ACS Omega 2022, 7, 23179−23188

Authors

Nilabja Maity − *Solid State and Structural Chemistry Unit, Indian Institute of Science, Bangalore 560012, India*

Kanad Majumder − *Solid State and Structural Chemistry Unit, Indian Institute of Science, Bangalore 560012, India;* orcid.org/0000-0001-7852-9105

Arun Kumar Patel − *NMR Research Centre, Indian Institute of Science, Bangalore 560012, India;* orcid.org/0000-0001-5949-4605

Diptikanta Swain − *Solid State and Structural Chemistry Unit, Indian Institute of Science, Bangalore 560012, India;* Present Address: Institute of Chemical Technology-Indian Oil Odisha Campus, Bhubaneswar, 751013, India; orcid.org/0000-0003-4048-5017

Nagarajarao Suryaprakash − *NMR Research Centre, Indian Institute of Science, Bangalore 560012, India;* orcid.org/0000-0002-9954-5195

Complete contact information is available at: https://pubs.acs.org/10.1021/acsomega.2c01091

Notes

The authors declare no competing financial interest.

■ ACKNOWLEDGMENTS

N.M. acknowledges CSIR and IISc Bangalore for a Senior Research Fellowship. S.P. thanks support from the EPSRC project Strategic University Network to Revolutionize Indian Solar Energy-SUNRISE (EP/P032591/1) and the Department of Science and Technology, New Delhi, for a Swarnajayanti Fellowship and SERB, IRHPA grant.

■ REFERENCES

(1) Hoeben, F. J. M.; Jonkheijm, P.; Meijer, E. W.; Schenning, A. P. H. J. About Supramolecular Assemblies of π-Conjugated Systems. *Chem. Rev.* **2005**, *105*, 1491−1546.

(2) Webber, M. J.; Appel, E. A.; Meijer, E. W.; Langer, R. Supramolecular Biomaterials. *Nat. Mater.* **2015**, *15*, 13−26.

(3) Wojtecki, R. J.; Meador, M. A.; Rowan, S. J. Using the Dynamic Bond to Access Macroscopically Responsive Structurally Dynamic Polymers. *Nat. Mater.* **2011**, *10*, 14−27.

(4) Zhang, S.; Greenfield, M. A.; Mata, A.; Palmer, L. C.; Bitton, R.; Mantei, J. R.; Aparicio, C.; De La Cruz, M. O.; Stupp, S. I. A Self-Assembly Pathway to Aligned Monodomain Gels. *Nat. Mater.* **2010**, *9*, 594−601.

(5) Fukushima, K.; Liu, S.; Wu, H.; Engler, A. C.; Coady, D. J.; Maune, H.; Pitera, J.; Nelson, A.; Wiradharma, N.; Venkataraman, S.; Huang, Y.; Fan, W.; Ying, J. Y.; Yang, Y. Y.; Hedrick, J. L. Supramolecular High-Aspect Ratio Assemblies with Strong Antifungal Activity. *Nat. Commun.* **2013**, *4*, 2861.

(6) Aida, T.; Meijer, E. W.; Stupp, S. I. Functional Supramolecular Polymers. *Science* **2012**, *335*, 813−817.

(7) Wu, J.; Pisula, W.; Müllen, K. Graphenes as Potential Material for Electronics. *Chem. Rev.* **2007**, *107*, 718−747.

(8) Schenning, A. P. H. J.; Meijer, E. W. Supramolecular Electronics; Nanowires from Self-Assembled π-Conjugated Systems. *Chem. Commun.* **2005**, *26*, 3245−3258.

(9) Yamamoto, Y.; Fukushima, T.; Suna, Y.; Ishii, N.; Saeki, A.; Seki, S.; Tagawa, S.; Taniguchi, M.; Kawai, T.; Aida, T. Photoconductive Coaxial Nanotubes of Molecularly Connected Electron Donor and Acceptor Layers. *Science* **2006**, *314*, 1761−1764.

(10) Babu, S. S.; Praveen, V. K.; Ajayaghosh, A. Functional π-Gelators and Their Applications. *Chem. Rev.* **2014**, *114*, 1973−2129.

(11) Hamlen, S. Advanced Materials. *Offshore Eng.* **2017**, *42*, 38−39.

(12) Lehn, J.-M. Perspectives in Supramolecular Chemistry—From Molecular Recognition towards Molecular Information Processing and Self-Organization. *Angew Chem. Int. Ed. Engl.* **1990**, *29*, 1304−1319.

(13) Lehn, J.-M. Toward Self-Organization and Complex Matter. *Science* **2002**, *295*, 2400−2403.

(14) Janssen, P. G. A.; Vandenbergh, J.; Van Dongen, J. L. J.; Meijer, E. W.; Schenning, A. P. H. J. J. SsDNA Templated Self-Assembly of Chromophores. *J. Am. Chem. Soc.* **2007**, *129*, 6078−6079.

(15) Mishra, A.; Korlepara, D. B.; Kumar, M.; Jain, A.; Jonnalagadda, N.; Bejagam, K. K.; Balasubramanian, S.; George, S. J. Biomimetic Temporal Self-Assembly via Fuel-Driven Controlled Supramolecular Polymerization. *Nat. Commun.* **2018**, *9*, 1295.

(16) Mishra, A.; Dhiman, S.; George, S. J. ATP-Driven Synthetic Supramolecular Assemblies: From ATP as a Template to Fuel. *Angew. Chem. Int. Ed.* **2021**, *60*, 2740−2756.

(17) Korevaar, P. A.; George, S. J.; Markvoort, A. J.; Smulders, M. M. J.; Hilbers, P. A. J.; Schenning, A. P. H. J.; De Greef, T. F. A.; Meijer, E. W. Pathway Complexity in Supramolecular Polymerization. *Nature* **2012**, *481*, 492−496.

(18) De Greef, T. F. A.; Smulders, M. M. J.; Wolffs, M.; Schenning, A. P. H. J.; Sijbesma, R. P.; Meijer, E. W. Supramolecular Polymerization. *Chem. Rev.* **2009**, *109*, 5687−5754.

(19) Bosman, A. W.; Janssen, H. M.; Meijer, E. W. About Dendrimers: Structure, Physical Properties, and Applications. *Chem. Rev.* **1999**, *99*, 1665−1688.

(20) Takata, T. Supramolecular Polymers. *Polymer* **2017**, *128*, 242.

(21) Yang, L.; Tan, X.; Wang, Z.; Zhang, X. Supramolecular Polymers: Historical Development, Preparation, Characterization, and Functions. *Chem. Rev.* **2015**, *115*, 7196−7239.

(22) Hirschberg, J. H. K. K.; Brunsveld, L.; Ramzi, A.; Vekemans, J. A. J. M.; Sijbesma, R. P.; Meijer, E. W. Helical Self-Assembled Polymers from Cooperative Stacking of Hydrogen-Bonded Pairs. *Nature* **2000**, *407*, 167−170.

(23) Sijbesma, R. P.; Beijer, F. H.; Brunsveld, L.; Folmer, B. J. B.; Hirschberg, J. H. K. K.; Lange, R. F. M.; Lowe, J. K. L.; Meijer, E. W. Reversible Polymers Formed from Self-Complementary Monomers Using Quadruple Hydrogen Bonding. *Science* **1997**, *278*, 1601−1604.

(24) Lutz, J.-F.; Lehn, J.-M.; Meijer, E. W.; Matyjaszewski, K. From Precision Polymers to Complex Materials and Systems. *Nat. Rev. Mater.* **2016**, *1*, 16024.

(25) Besenius, P.; Portale, G.; Bomans, P. H. H.; Janssen, H. M.; Palmans, A. R. A.; Meijer, E. W. Controlling the Growth and Shape of Chiral Supramolecular Polymers in Water. *Proc. Natl. Acad. Sci. U. S. A.* **2010**, *107*, 17888−17893.

(26) Ten Cate, A. T.; Kooijman, H.; Spek, A. L.; Sijbesma, R. P.; Meijer, E. W. Conformational Control in the Cyclization of Hydrogen-Bonded Supramolecular Polymers. *J. Am. Chem. Soc.* **2004**, *126*, 3801−3808.

(27) Ligthart, G. B. W. L.; Ohkawa, H.; Sijbesma, R. P.; Meijer, E. W. Complementary Quadruple Hydrogen Bonding in Supramolecular Copolymers. *J. Am. Chem. Soc.* **2005**, *127*, 810−811.

(28) Lee, J. Y.; Olson, D. H.; Pan, L.; Emge, T. J.; Li, J. Microporous Metal-Organic Frameworks with High Gas Sorption and Separation Capacity. *Adv. Funct. Mater.* **2007**, *17*, 1255−1262.

(29) Yamamoto, Y.; Zhang, G.; Jin, W.; Fukushima, T.; Ishii, N.; Saeki, A.; Seki, S.; Tagawa, S.; Minari, T.; Tsukagoshi, K.; Aida, T. Ambipolar-Transporting Coaxial Nanotubes with a Tailored Molecular Graphene - Fullerene Heterojunction. *Proc. Natl. Acad. Sci. U.S.A.* **2009**, *106*, 21051−21056.

(30) Haedler, A. T.; Kreger, K.; Issac, A.; Wittmann, B.; Kivala, M.; Hammer, N.; Köhler, J.; Schmidt, H.-W.; Hildner, R. Long-Range Energy Transport in Single Supramolecular Nanofibres at Room Temperature. *Nature* **2015**, *523*, 196−199.

(31) Percec, V.; Glodde, M.; Bera, T. K.; Miura, Y.; Shiyanovskaya, I.; Singer, K. D.; Balagurusamy, V. S. K.; Heiney, P. A.; Schnell, I.; Rapp, A.; Spiess, H.-W.; Hudson, S. D.; Duan, H. Self-Organization

of Supramolecular Helical Dendrimers into Complex Electronic Materials. *Nature* **2002**, *419*, 384−387.
(32) Rao, K. V.; Jayaramulu, K.; Maji, T. K.; George, S. J. Supramolecular Hydrogels and High-Aspect-Ratio Nanofibers through Charge-Transfer-Induced Alternate Coassembly. *Angew. Chem.* **2010**, *122*, 4314−4318.
(33) Herz, M.; Daniel, C.; Silva, C.; Hoeben, M.; Schenning, H. J.; Meijer, W.; Friend, H.; Phillips, T. Fast Exciton Diffusion in Chiral Stacks of Conjugated P-Phenylene Vinylene Oligomers. *Phys. Rev. B Condens. Matter* **2003**, *68*, 045203.
(34) Wolffs, M.; Hoeben, F. J. M.; Beckers, E. H. A.; Schenning, A. P. H. J.; Meijer, E. W. Sequential Energy and Electron Transfer in Aggregates of Tetrakis[Oligo(p-Phenylene Vinylene)] Porphyrins and C60 in Water. *J. Am. Chem. Soc.* **2005**, *127*, 13484−13485.
(35) Van Herrikhuyzen, J.; Syamakumari, A.; Schenning, A. P. H. J.; Meijer, E. W. Synthesis of N-Type Perylene Bisimide Derivatives and Their Orthogonal Self-Assembly with p-Type Oligo(p-Phenylene Vinylene)S. *J. Am. Chem. Soc.* **2004**, *126*, 10021−10027.
(36) Miura, A.; Chen, Z.; Uji-I, H.; De Feyter, S.; Zdanowska, M.; Jonkheijm, P.; Schenning, A. P. H. J.; Meijer, E. W.; Würthner, F.; De Schryver, F. C. Bias-Dependent Visualization of Electron Donor (D) and Electron Acceptor (A) Moieties in a Chiral DAD Triad Molecule. *J. Am. Chem. Soc.* **2003**, *125*, 14968−14969.
(37) Würthner, F.; Chen, Z.; Hoeben, F. J. M.; Osswald, P.; You, C.-C.; Jonkheijm, P.; Herrikhuyzen, J. V.; Schenning, A. P. H. J.; Van Der Schoot, P. P. A. M.; Meijer, E. W.; Beckers, E. H. A.; Meskers, S. C. J.; Janssen, R. A. J. J. Supramolecular P-n-Heterojunctions by Co-Self-Organization of Oligo(p-Phenylene Vinylene) and Perylene Bisimide Dyes. *J. Am. Chem. Soc.* **2004**, *126*, 10611−10618.
(38) Sakakibara, K.; Chithra, P.; Das, B.; Mori, T.; Akada, M.; Labuta, J.; Tsuruoka, T.; Maji, S.; Furumi, S.; Shrestha, L. K.; Hill, J. P.; Acharya, S.; Ariga, K.; Ajayaghosh, A. Aligned 1-D Nanorods of a π-Gelator Exhibit Molecular Orientation and Excitation Energy Transport Different from Entangled Fiber Networks. *J. Am. Chem. Soc.* **2014**, *136*, 8548−8551.
(39) Prasanthkumar, S.; Saeki, A.; Seki, S.; Ajayaghosh, A. Solution Phase Epitaxial Self-Assembly and High Charge-Carrier Mobility Nanofibers of Semiconducting Molecular Gelators. *J. Am. Chem. Soc.* **2010**, *132*, 8866−8867.
(40) Prasanthkumar, S.; Gopal, A.; Ajayaghosh, A. Self-Assembly of Thienylenevinylene Molecular Wires to Semiconducting Gels with Doped Metallic Conductivity. *J. Am. Chem. Soc.* **2010**, *132*, 13206−13207.
(41) Jiang, J.; Xu, Z.; Zhou, J.; Hanif, M.; Jiang, Q.; Hu, D.; Zhao, R.; Wang, C.; Liu, L.; Ma, D.; Ma, Y.; Cao, Y. Enhanced Pi Conjugation and Donor/Acceptor Interactions in D-A-D Type Emitter for Highly Efficient Near-Infrared Organic Light-Emitting Diodes with an Emission Peak at 840 nm. *Chem. Mater.* **2019**, *31*, 6499−6505.
(42) Praveen, V. K.; Vedhanarayanan, B.; Mal, A.; Mishra, R. K.; Ajayaghosh, A. Self-Assembled Extended π-Systems for Sensing and Security Applications. *Acc. Chem. Res.* **2020**, *53*, 496−507.
(43) Crone, B.; Dodabalapur, A.; Lin, Y.-Y.; Filas, R. W.; Bao, Z.; LaDuca, A.; Sarpeshkar, R.; Katz, H. E.; Li, W. Large-Scale Complementary Integrated Circuits Based on Organic Transistors. *Nature* **2000**, *403*, 521−523.
(44) Zhou, W.; Kuebler, S. M.; Braun, K. L.; Yu, T.; Cammack, J. K.; Ober, C. K.; Perry, J. W.; Marder, S. R. An Efficient Two-Photon-Generated Photoacid Applied to Positive-Tone 3D Microfabrication. *Science* **2002**, *296*, 1106−1109.
(45) Cumpston, B. H.; Ananthavel, S. P.; Barlow, S.; Dyer, D. L.; Ehrlich, J. E.; Erskine, L. L.; Heikal, A. A.; Lee, I.-Y. S.; McCord-Maughon, D.; Qin, J.; Röckel, H.; Wu, X.-L.; Marder, S. R.; Perry, J. W. Two-Photon Polymerization Initiators for Three-Dimensional Optical Data Storage and Microfabrication. *Nature* **1999**, *398*, 51−54.
(46) Ahn, M.; Kim, M.-J.; Wee, K.-R. Electron Push-Pull Effects in 3,9-Bis(p-(R)-Diphenylamino)Perylene and Constraint on Emission Color Tuning. *J. Org. Chem.* **2019**, *84*, 12050−12057.
(47) Yuan, J.; Zhang, Y.; Zhou, L.; Zhang, G.; Yip, H. L.; Lau, T. K.; Lu, X.; Zhu, C.; Peng, H.; Johnson, P. A.; Leclerc, M.; Cao, Y.; Ulanski, J.; Li, Y.; Zou, Y. Single-Junction Organic Solar Cell with over 15% Efficiency Using Fused-Ring Acceptor with Electron-Deficient Core. *Joule* **2019**, *3*, 1140−1151.
(48) Mei, J.; Diao, Y.; Appleton, A. L.; Fang, L.; Bao, Z. Integrated Materials Design of Organic Semiconductors for Field-Effect Transistors. *J. Am. Chem. Soc.* **2013**, *135*, 6724−6746.
(49) Pawlicki, M.; Collins, H. A.; Denning, R. G.; Anderson, H. L. Two-Photon Absorption and the Design of Two-Photon Dyes. *Angew. Chem. Int. Ed.* **2009**, *48*, 3244−3266.
(50) Allen, T. G.; Benis, S.; Munera, N.; Zhang, J.; Dai, S.; Li, T.; Jia, B.; Wang, W.; Barlow, S.; Hagan, D. J.; Van Stryland, E. W.; Zhan, X.; Perry, J. W.; Marder, S. R. Highly Conjugated, Fused-Ring, Quadrupolar Organic Chromophores with Large Two-Photon Absorption Cross-Sections in the Near-Infrared. *J. Phys. Chem. A* **2020**, *124*, 4367−4378.
(51) Albota, M.; Beljonne, D.; Brédas, J.-L.; Ehrlich, J. E.; Fu, J.-Y.; Heikal, A. A.; Hess, S. E.; Kogej, T.; Levin, M. D.; Marder, S. R.; McCord-Maughon, D.; Perry, J. W.; Röckel, H.; Rumi, M.; Subramaniam, G.; Webb, W. W.; Wu, X.-L.; Xu, C. Design of Organic Molecules with Large Two-Photon Absorption Cross Sections. *Science* **1998**, *281*, 1653−1656.
(52) Fedoseeva, M.; Letrun, R.; Vauthey, E. Excited-State Dynamics of Rhodamine 6G in Aqueous Solution and at the Dodecane/Water Interface. *J. Phys. Chem. B* **2014**, *118*, 5184−5193.
(53) Liu, Q.; Bottle, S. E.; Sonar, P. Developments of Diketopyrrolopyrrole-Dye-Based Organic Semiconductors for a Wide Range of Applications in Electronics. *Adv. Mater.* **2020**, *32*, 1903882.
(54) Bao, W. W.; Li, R.; Dai, Z. C.; Tang, J.; Shi, X.; Geng, J. T.; Deng, Z. F.; Hua, J. Diketopyrrolopyrrole (DPP)-Based Materials and Its Applications: A Review. *Front. Chem.* **2020**, *8*, 679.
(55) Zou, X.; Cui, S.; Li, J.; Wei, X.; Zheng, M. Diketopyrrolopyrrole Based Organic Semiconductor Materials for Field-Effect Transistors. *Front. Chem.* **2021**, *9*. DOI: 10.3389/fchem.2021.671294
(56) Ghosh, S.; Cherumukkil, S.; Suresh, C. H.; Ajayaghosh, A. A Supramolecular Nanocomposite as a Near-Infrared-Transmitting Optical Filter for Security and Forensic Applications. *Adv. Mater.* **2017**, *29*. DOI: 10.1002/adma.201703783
(57) Guzman, C. X.; Calderon, R. M. K.; Li, Z.; Yamazaki, S.; Peurifoy, S. R.; Guo, C.; Davidowski, S. K.; Mazza, M. M. A.; Han, X.; Holland, G.; Scott, A. M.; Braunschweig, A. B. Extended Charge Carrier Lifetimes in Hierarchical Donor−Acceptor Supramolecular Polymer Films. *J. Phys. Chem. C* **2015**, *119*, 19584−19589.
(58) Rieth, S.; Li, Z.; Hinkle, C. E.; Guzman, C. X.; Lee, J. J.; Nehme, S. I.; Braunschweig, A. B. Superstructures of Diketopyrrolopyrrole Donors and Perylenediimide Acceptors Formed by Hydrogen-Bonding and π ···π Stacking. *J. Phys. Chem. C* **2013**, *117*, 11347−11356.
(59) Ley, D.; Guzman, C. X.; Adolfsson, K. H.; Scott, A. M.; Braunschweig, A. B. Cooperatively Assembling Donor-Acceptor Superstructures Direct Energy into an Emergent Charge Separated State. *J. Am. Chem. Soc.* **2014**, *136*, 7809−7812.
(60) Draper, E. R.; Dietrich, B.; Adams, D. J. Self-Assembly, Self-Sorting, and Electronic Properties of a Diketopyrrolopyrrole Hydrogelator. *Chem. Commun.* **2017**, *53*, 1864−1867.
(61) Song, B.; Wei, H.; Wang, Z.; Zhang, X.; Smet, M.; Dehaen, W. Supramolecular Nanofibers by Self-Organization of Bola-Amphiphiles through a Combination of Hydrogen Bonding and π-π Stacking Interactions. *Adv. Mater.* **2007**, *19*, 416−420.
(62) Ruiz-Carretero, A.; Ávila Rovelo, N. R.; Militzer, S.; Mésini, P. J. Hydrogen-Bonded Diketopyrrolopyrrole Derivatives for Energy-Related Applications. *J. Mater. Chem. A* **2019**, *7*, 23451−23475.

https://doi.org/10.1021/acsomega.2c01091
ACS Omega 2022, 7, 23179−23188

(63) Ogi, S.; Fukaya, N.; Arifin; Skjelstad, B. B.; Hijikata, Y.; Yamaguchi, S. Seeded Polymerization of an Amide-Functionalized Diketopyrrolopyrrole Dye in Aqueous Media. *Chem. Eur J.* **2019**, *25*, 7303−7307.
(64) Kirkus, M.; Wang, L.; Mothy, S.; Beljonne, D.; Cornil, J.; Janssen, R. A. J.; Meskers, S. C. J. Optical Properties of Oligothiophene Substituted Diketopyrrolopyrrole Derivatives in the Solid Phase: Joint J- and H-Type Aggregation. *J. Phys. Chem. A* **2012**, *116*, 7927−7936.
(65) Hartnett, P. E.; Margulies, E. A.; Mauck, C. M.; Miller, S. A.; Wu, Y.; Wu, Y.-L.; Marks, T. J.; Wasielewski, M. R. Effects of Crystal Morphology on Singlet Exciton Fission in Diketopyrrolopyrrole Thin Films. *J. Phys. Chem. B* **2016**, *120*, 1357−1366.
(66) Luo, N.; Zhang, G.; Liu, Z. Keep Glowing and Going: Recent Progress in Diketopyrrolopyrrole Synthesis towards Organic Optoelectronic Materials. *Org. Chem. Front.* **2021**, *8*, 4560−4581.
(67) Zhao, C.; Guo, Y.; Zhang, Y.; Yan, N.; You, S.; Li, W. Diketopyrrolopyrrole-Based Conjugated Materials for Non-Fullerene Organic Solar Cells. *J. Mater. Chem. A* **2019**, *7*, 10174−10199.
(68) Tang, A.; Zhan, C.; Yao, J.; Zhou, E. Design of Diketopyrrolopyrrole (DPP)-Based Small Molecules for Organic-Solar-Cell Applications. *Adv. Mater.* **2017**, *29*, 1600013.
(69) Yi, Z.; Wang, S.; Liu, Y. Design of High-Mobility Diketopyrrolopyrrole-Based π-Conjugated Copolymers for Organic Thin-Film Transistors. *Adv. Mater.* **2015**, *27*, 3589−3606.
(70) Nielsen, C. B.; Turbiez, M.; McCulloch, I. Recent Advances in the Development of Semiconducting DPP-Containing Polymers for Transistor Applications. *Adv. Mater.* **2013**, *25*, 1859−1880.
(71) Mei, J.; Graham, K. R.; Stalder, R.; Tiwari, S. P.; Cheun, H.; Shim, J.; Yoshio, M.; Nuckolls, C.; Kippelen, B.; Castellano, R. K.; Reynolds, J. R. Self-Assembled Amphiphilic Diketopyrrolopyrrole-Based Oligothiophenes for Field-Effect Transistors and Solar Cells. *Chem. Mater.* **2011**, *23*, 2285−2288.
(72) Zhao, W.; Ding, J.; Zou, Y.; Di, C.-a.; Zhu, D. Chemical Doping of Organic Semiconductors for Thermoelectric Applications. *Chem. Soc. Rev.* **2020**, *49*, 7210−7228.
(73) Samuel, J. J.; Garudapalli, A.; Mohapatra, A. A.; Gangadharappa, C.; Patil, S.; Aetukuri, N. P. B. Single-Component CMOS-Like Logic Using Diketopyrrolopyrrole-Based Ambipolar Organic Electrochemical Transistors. *Adv. Funct. Mater.* **2021**, 2102903.
(74) Kanimozhi, C.; Balraju, P.; Sharma, G. D.; Patil, S. Synthesis of Diketopyrrolopyrrole Containing Copolymers: A Study of Their Optical and Photovoltaic Properties. *J. Phys. Chem. B* **2010**, *114*, 3095−3103.
(75) Naik, M. A.; Venkatramaiah, N.; Kanimozhi, C.; Patil, S. Influence of Side-Chain on Structural Order and Photophysical Properties in Thiophene Based Diketopyrrolopyrroles: A Systematic Study. *J. Phys. Chem. C* **2012**, *116*, 26128−26137.
(76) Dhar, J.; Venkatramaiah, N.; Patil, S. Photophysical Electrochemical and Solid State Properties of Diketopyrrolopyrrole Based Molecular Materials: Importance of the Donor Group. *J. Mater. Chem. C* **2014**, *2*, 3457−3466.
(77) Mukhopadhyay, T.; Puttaraju, B.; Roy, P.; Dasgupta, J.; Meyer, A.; Rudnick, A.; Tscheuschner, S.; Kahle, F.-J.; Köhler, A.; Patil, S. Facile Synthesis and Chain-Length Dependence of the Optical and Structural Properties of Diketopyrrolopyrrole-Based Oligomers. *Chem. Eur J.* **2017**, *23*, 13718−13723.
(78) Ray, S.; Panidi, J.; Mukhopadhyay, T.; Salzner, U.; Anthopoulos, T. D.; Patil, S. Electrochemical Stability and Ambipolar Charge Transport in Diketopyrrolopyrrole-Based Organic Materials. *ACS Appl. Electron. Mater.* **2019**, *1*, 2037−2046.
(79) Kanimozhi, C.; Yaacobi-Gross, N.; Chou, K. W.; Amassian, A.; Anthopoulos, T. D.; Patil, S. Diketopyrrolopyrrole-Diketopyrrolopyrrole-Based Conjugated Copolymer for High-Mobility Organic Field-Effect Transistors. *J. Am. Chem. Soc.* **2012**, *134*, 16532−16535.
(80) Senanayak, S. P.; Ashar, A. Z.; Kanimozhi, C.; Patil, S.; Narayan, K. S. Room-Temperature Bandlike Transport and Hall Effect in a High-Mobility Ambipolar Polymer. *Phys. Rev. B Condens. Matter* **2015**, *91*, 115302.
(81) Ghosh, S.; Philips, D. S.; Saeki, A.; Ajayaghosh, A. Nanosheets of an Organic Molecular Assembly from Aqueous Medium Exhibit High Solid-State Emission and Anisotropic Charge-Carrier Mobility. *Adv. Mater.* **2017**, *29*, 1605408.
(82) Berl, V.; Schmutz, M.; Krische, M. J.; Khoury, R. G.; Lehn, J.-M. Supramolecular Polymers Generated from Heterocomplementary Monomers. *Chem. - Eur. J.* **2002**, *8*, 1227−1244.
(83) Chang, S. K.; Hamilton, A. D. Molecular Recognition of Biologically Interesting Substrates: Synthesis of an Artificial Receptor for Barbiturates Employing Six Hydrogen Bonds. *J. Am. Chem. Soc.* **1988**, *110*, 1318−1319.
(84) Gershberg, J.; Fennel, F.; Rehm, T. H.; Lochbrunner, S.; Würthner, F. Anti-Cooperative Supramolecular Polymerization: A New K 2 −K Model Applied to the Self-Assembly of Perylene Bisimide Dye Proceeding via Well-Defined Hydrogen-Bonded Dimers. *Chem. Sci.* **2016**, *7*, 1729−1737.
(85) Kolomiets, E.; Buhler, E.; Candau, S. J.; Lehn, J.-M. Structure and Properties of Supramolecular Polymers Generated from Heterocomplementary Monomers Linked through Sextuple Hydrogen-Bonding Arrays. *Macromolecules* **2006**, *39*, 1173−1181.
(86) Schmidt, R.; Stolte, M.; Grüne, M.; Würthner, F. Hydrogen-Bond-Directed Formation of Supramolecular Polymers Incorporating Head-to-Tail Oriented Dipolar Merocyanine Dyes. *Macromolecules* **2011**, *44*, 3766−3776.
(87) Data, P.; Kurowska, A.; Pluczyk, S.; Zassowski, P.; Pander, P.; Jedrysiak, R.; Czwartosz, M.; Otulakowski, L.; Suwinski, J.; Lapkowski, M.; Monkman, A. P. Exciplex Enhancement as a Tool to Increase OLED Device Efficiency. *J. Phys. Chem. C* **2016**, *120*, 2070−2078.
(88) Chaudhari, S. R.; Suryaprakash, N. Diffusion Ordered Spectroscopy for Resolution of Double Bonded Cis, Trans-Isomers. *J. Mol. Struct.* **2012**, *1017*, 106−108.
(89) Chaudhari, S. R.; Srinivasa; Suryaprakash, N. Cyclodextrin and Its Complexation for Resolution of Isomers Using Diffusion Ordered Spectroscopy. *J. Mol. Struct.* **2013**, *1033*, 75−78.
(90) Folmer, B. J. B.; Sijbesma, R. P.; Meijer, E. W. Unexpected Entropy-Driven Ring-Opening Polymerization in a Reversible Supramolecular System. *J. Am. Chem. Soc.* **2001**, *123*, 2093−2094.

https://doi.org/10.1021/acsomega.2c01091
ACS Omega 2022, 7, 23179−23188